Eur. Phys. J. B **43**, 201–212 (2005)
DOI: 10.1140/epjb/e2005-00043-5

THE EUROPEAN PHYSICAL JOURNAL B

Magnetic AC susceptibility of stoichiometric and low zinc doped magnetite single crystals

M. Bałanda[2], A. Wiecheć[1], D. Kim[3], Z. Kąkol[1,a], A. Kozłowski[1], P. Niedziela[1], J. Sabol[5,b], Z. Tarnawski[1], and J.M. Honig[4]

[1] Faculty of Physics and Applied Computer Science, AGH-University of Science and Technology, Kraków, Poland
[2] Institute of Nuclear Physics, Kraków, Poland
[3] Department of Chemistry, Pukyong National University, Pusan 608-737, Korea
[4] Department of Chemistry, Purdue University, West Lafayette, Indiana, USA
[5] Department of Geology and Geophysics, University of Wisconsin-Madison, USA

Received 25 September 2004
Published online 25 February 2005 –

Abstract. Systematic studies of AC susceptibility in a stoichiometric magnetite single crystal, in a series of low zinc doped magnetite ($x_{\mathrm{Zn}} < 0.04$) and in nonstoichiometric magnetite samples (both single crystals and pellets) in the temperature range 4–300 K are presented. Measurements were performed in several AC fields ($H_{AC} = 0.2-20$ Oe) and at different frequencies (15–6000 Hz). It is suggested that the signal is primarily due to magnetic domain wall movement, strongly influenced by structural domains (twins). Two sets of anomalies were found: the first is associated with the Verwey transition and the second involves two different effects, one at 28 K, observed only in stoichiometric magnetite, and the other at 50 K. While the temperature position of the first anomaly (28 K) does not depend on frequency, the effect at 50 K is associated with an activation process, shifting to higher temperatures with increasing frequency. This last effect may be linked to the low temperature magnetoelectric effects terminating approximately at those temperatures. Qualitatively similar results have been observed by the Magnetic After Effect technique presented in the literature, that is associated with relaxation times that are 10^4 higher than those characteristic of our technique.

PACS. 71.30.+h Metal-insulator transitions and other electronic transitions – 75.30.Cr Saturation moments and magnetic susceptibilities – 75.60.-d Domain effects, magnetization curves, and hysteresis

1 Introduction

In this paper we present dynamic magnetic susceptibility measurements on low doped zinc ferrite $Fe_{3-x}Zn_xO_4$ and nonstoichiometric magnetite $Fe_{3(1-\delta)}O_4$ samples at temperatures both above and below the Verwey transition. We encountered several low temperature (T) anomalies, most of them of relaxation character, that gradually disappear with increasing Zn content or with increasing departures from stoichiometry. A discussion of the origin of those anomalies is presented. These results constitute part of a wider project dealing with interactions relevant to the Verwey transition, in particular, magnetic interactions, and changes in the character of this transition with doping.

Magnetite is well known for its extensive use in traditional recording media and for its role in the emerging field of spintronics [1]. This material has been the focus of much work in this area over the last 60 years (for a recent overview and a comprehensive search of literature refer to e.g. [2] or to [3]), due to the discontinuous Verwey phase transformation at $T_V = 124$ K, where the resistivity increases abruptly by two orders of magnitude and the structure changes from cubic (Fd3m inverse spinel lattice) to monoclinic below T_V.

Many properties of magnetite, in particular the details of the Verwey transition, were linked to the presence of Fe^{+3} and Fe^{+2} ions on octahedral cationic positions in the lattice that are not differentiated when the crystal is heated above T_V. Thus, while the electrons were considered frozen on particular, although still unknown, positions at low T, generating specific Fe^{+2} and Fe^{+3} cations, they were regarded as being equally spread across all octahedral Fe positions above the Verwey transition, thus setting up the intermediate $Fe^{+2.5}$ valence state. Anderson [4] suggested that the electron motion is highly influenced by strong, interionic Coulomb interactions that

[a] e-mail: kakol@uci.agh.edu.pl
[b] *Present address*: Sabol Consulting Services, 316 Harrison St. Marquette, MI 49855-3316

primarily drive the transition. However, Coulomb repulsions, together with the peculiarity of the structure, gives rise to many energy degeneracies in possible cationic patterns that develop below T_V. Hence, additional, much smaller, interactions were postulated to exist that stabilize long-range order. Since the problem of finding those additional interactions is not entirely solved, and since magnetic interactions were sometimes invoked, studies of magnetic properties are still needed. This is the primary reason why we engaged in the present study.

Although many phenomena relating to magnetite may by explained by adopting the simple ionic picture [2] outlined above, other measurements show that the real mechanism is much more complicated [3]. For example, NMR [5] and anomalous X ray diffraction studies [6] suggest that the low T electronic states of the two sets of octahedral Fe ions are very similar, rendering the usual interpretation of phenomena in terms of Fe^{2+} and Fe^{3+} states highly questionable. Also, the dominance of interionic Coulomb interactions has been questioned [7], and no high T electron hopping times below 10^{-16} s have been found [6]. This is in accord with recent Mössbauer studies [8] showing that above the coordination crossover temperature T_{CC}, equal to T_V at ambient pressure, but much higher when external pressure is applied, all octahedral positions are occupied by Fe^{+3} ions, so that magnetite then becomes a normal spinel. Recent band structure calculations [9], based on Local Spin Density method with the self-interaction term removed, support this conjecture.

Magnetic properties of Fe_3O_4 should also reflect the electronic arrangement and thus may be usefully studied to determine the dominant mechanism of the transition. At high temperatures the magnetic easy, intermediate and hard axes lie along cubic $\langle 111 \rangle$, $\langle 110 \rangle$ and $\langle 001 \rangle$ directions, respectively. The situation changes at the isotropy point of $T_{IP} = 130$ K (where the dominant anisotropy constant K_1 diminishes to zero); below this temperature the magnetic moment points along the $\langle 100 \rangle$ direction [5,10]. This easy direction is preserved below T_V, where the cubic symmetry changes to monoclinic. Here, with no significant, (less than 0.1% [11,12]), change in magnetization, a drastic increase in magnetic anisotropy energy occurs [13,14], so that each cubic $\langle 100 \rangle$ becomes an easy axis. This causes the material to break into several structural domains (twins) unless an external magnetic field $H > 2$ kOe along particular [001] is applied [15,14]. On the other hand, once a particular easy axis has been established and the magnetite sample is magnetized along some other $\langle 100 \rangle$ direction, then at temperatures T_{AS}, slightly lower than T_V, a reorientation of magnetic moments, i.e. axis switching, may take place. This particular $\langle 100 \rangle$ direction then becomes a new easy axis. Since the effect is probably linked to a relaxation of entities that order at T_V, the observation of axis switching provides a unique possibility to study the onset of ordering prior to the actual transformation.

The Verwey transition may be finely tuned by the departures from stoichiometry or by controlled doping e.g. with Zn. Namely, if 3δ in $Fe_{3(1-\delta)}O_4$ [16] or x in $Fe_{3-x}Zn_xO_4$ [17] is less than 0.012, then a first order Verwey transition is observed, with a linear decrease of T_V. Above this concentration the transition is continuous, with a different linear T_V vs. 3δ or x relation. Despite the numerous investigations the change in order of the transition has never been fully explained.

Bearing in mind all the above facts, in particular the unclear role of magnetic interactions, and the still vague ordering process influencing magnetic characteristics, it is evident that precise magnetic measurements would contribute to an understanding of properties of this material. For that reason we have found it appropriate to study the magnetic properties of $Fe_{3-x}Zn_xO_4$ single crystals by means of AC susceptibility. This technique was proved to be successful for study the systems containing magnetic ions in two valence states [2,18]. In particular, it was also applied for manganites where the electronic sub-micrometer scale phase separation, possibly responsible for colossal magnetoresistance effects, was linked to Mn valence instabilities [19]. Interestingly, as in magnetite, also in this class of materials the strict ionic order was recently questioned [20].

A nonstoichiometric magnetite crystal, as well as pellet samples, were measured for comparison. By this means we have complemented previous AC susceptibility studies of magnetite by Skumryev et al. [21]. Parts of our results have already been presented [22].

Our measurements on stoichiometric magnetite revealed a pronounced dip at $28 < T < 50$ K that actually consists of at least two different contributions, one at 28 K and the other at 50 K. While the temperature position of the first anomaly (28 K) does not depend on the applied AC frequency, the effect at 50 K shifts to higher temperatures with increasing frequency. The influence of the H_{AC} amplitude on those anomalies is also found and will be discussed, and the effect of field cooling and external field on χ_{AC} for all studied samples will be presented. Note that Magnetic After Effect (MAE) anomalies [2] occur in exactly the same temperature region as our observations, despite the fact that MAE is sensitive to processes with much longer characteristic time scales than ours.

The experimental details and the results of our measurements are presented in Sections 2 and 3. The dominant mechanism of the magnetic susceptibility response in magnetite and all anomalies found are discussed in Section 4 under appropriate headings. Conclusions are presented in Section 5.

2 Experiment

Single crystalline magnetite $Fe_{3(1-\delta)}O_4$ ($\delta = 0$ – two samples and $\delta = 0.009$), as well as zinc ferrites $Fe_{3-x}Zn_xO_4$, ($x = 0.0072$, 0.0174 and 0.049) samples, were grown from the melt, using the cold crucible technique (skull melter) [23], at Purdue University, USA. The crystals were then subjected to subsolidus annealing under CO/CO_2 gas mixtures to establish the appropriate metal/oxygen ratio [24], and rapidly quenched to room temperature to freeze in the high temperature thermodynamic equilibrium. Although this procedure generates octahedral

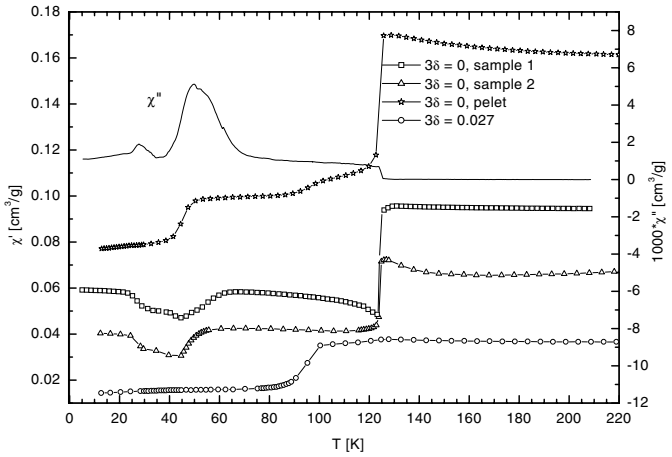

Fig. 1. Temperature dependence of in-phase susceptibility (left scale) for magnetite samples $Fe_{3(1-\delta)}O_4$. The experimental conditions were: $f = 125$ Hz, $H_{AC} = 1$ Oe. The data for the sample 1 (for which also out-of-plane component is presented; line) is shifted 0.02 cm^3/g upward for clarity.

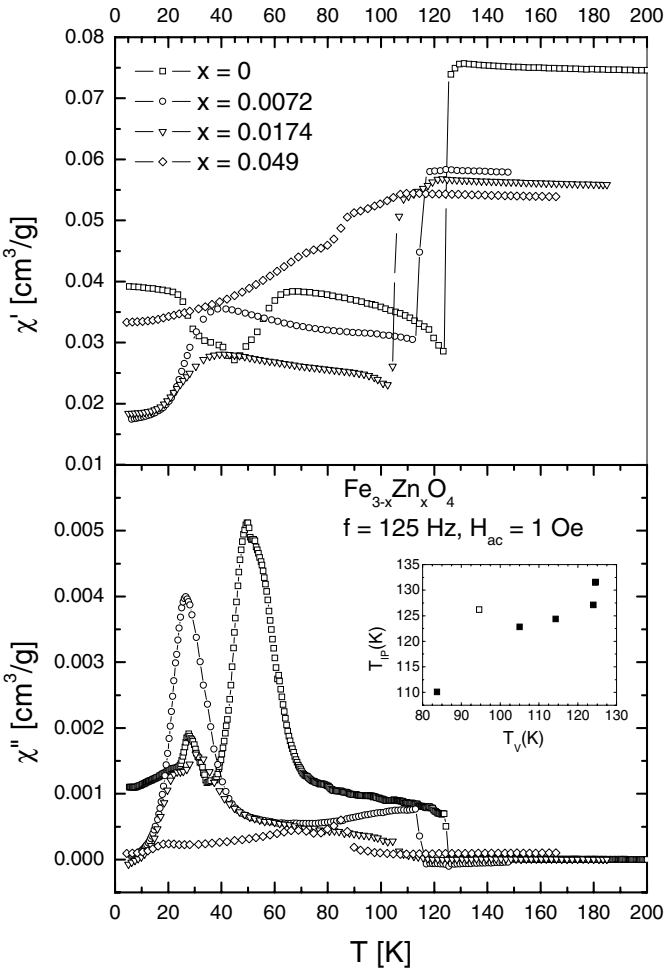

Fig. 2. Temperature dependence of susceptibility for zinc ferrite samples. The data for $x = 0$ (sample 1) are also shown. The inset presents the correlation between the isotropy point temperature T_{IS} and T_V; here the open symbol refers to the nonstoichiometric sample.

defects [2] that reflect the high T disorder, most of low temperature electronic processes are not thereby spoiled, as is evidenced by the sharp transition and high Verwey transition temperature. For two samples, the actual composition and sample uniformity were checked with a microprobe electron analyzer, while for one sample, $x = 0.0072$, the composition was estimated from the universal T_V vs. x curve [25]. After preparation the crystals were first oriented by the Laue method and then cut into cubes of typical dimension $1 \times 1 \times 1$ mm^3, exposing two (110) and one (100) surfaces. Pressed pellets of polycrystalline magnetite were also annealed under appropriate CO/CO_2 gas mixtures and drop-quenched to liquid nitrogen temperatures to achieve the intended δ in $Fe_{3(1-\delta)}O_4$.

The AC susceptibility was measured on commercial LakeShore ACS7000 series susceptometers in two separate laboratories (all samples were measured in Kraków, except for two magnetite crystals (sample 2, and the nonstoichiometric sample with $3\delta = 0.027$), and the pellet, which were measured in Pusan) in the temperature range 4.2–300 K, in an AC magnetic field of amplitude 0.2 Oe to 20 Oe, and in an applied frequency range from 15 Hz to 6000 Hz. The [001] crystallographic direction of bulk single crystals was set parallel to the H_{AC} direction.

The in-phase, χ' and out-of-phase, χ'', components of the AC susceptibility, $\chi_{AC} = \chi' - i\chi''$ were recorded while heating the sample, both after zero-field cooling (ZFC) and after field-cooling (FC). For some samples the measurements were also performed with the external magnetic field set parallel to [001].

3 Results

The in-phase components χ' of the AC susceptibility χ_{AC} measured at $f = 125$ Hz and $H_{AC} = 1$ Oe for magnetite samples (both stoichiometric and nonstoichiometric) are presented in Figure 1. The complete data for Zn doped magnetite (including the $x = 0$, sample 1, for comparison) and for both in-phase χ' and absorption χ'' components are shown in Figure 2. Two regimes in the shape of the Verwey transition, are clearly observed: stoichiometric magnetite and the specimen with $x = 0.0072$ undergo first order transitions, while for $x = 0.049$ the transition is continuous. The sample with $x = 0.0174$, being in the higher order regime, as judged by the universal T_V vs. Zn content relation [25], displays a relatively sharp Verwey transition at $T = 105$ K as judged by the χ' vs. T variation, but is apparently of continuous character according to the χ'' vs. T dependence. The most evident and universal conclusion derived from the curves in Figures 1 and 2 is that much more energy is lost in maneuvering the spins below than above the Verwey transition.

Anomalous behavior is encountered in χ_{AC} measurements below 70 K in all samples: χ' increases during heating, which is reflected in the simultaneous peak in χ'' (for $x = 0.049$ only a small peak in χ'' is seen). In stoichiometric magnetite this increase is preceded by a drop of χ', exhibiting a characteristic subtle structure until high T values are reached. Mostly featureless behavior is found at

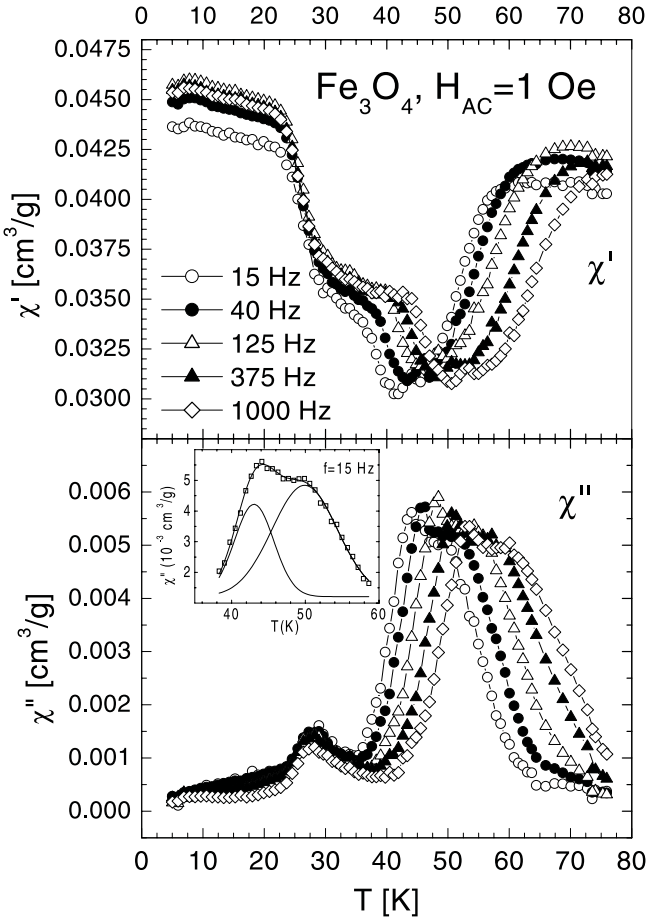

Fig. 3. Temperature dependence of low T susceptibility for $x = 0$ and for several frequencies ($H_{AC} = 1$ Oe). The inset shows the typical breaking of anomaly in T range 40–60 K into two peaks.

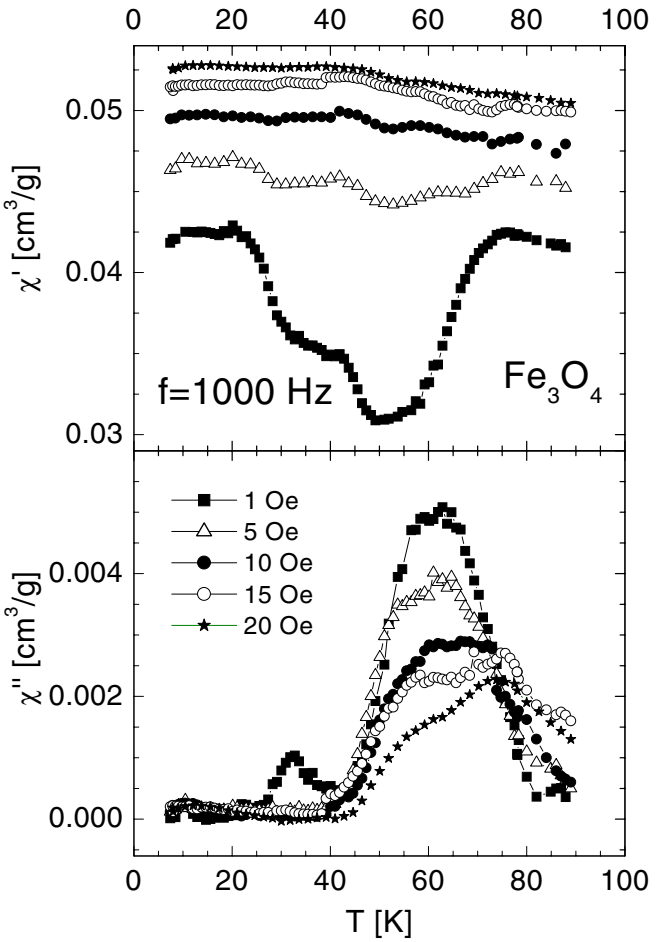

Fig. 4. Temperature dependence of low T susceptibility for $x = 0$, $f = 1000$ Hz and for several driving fields H_{AC}.

low temperatures for other samples, suggesting that the peculiar χ_{AC} shape depends critically on the quality and composition of the crystals. As already reported [2,21,22], χ' changes discontinuously at T_V, with a simultaneous drop in the loss function χ''; these features at T_V do not depend on the frequency of the driving field. There is a clear kink in χ' just above the Verwey transition that probably coincides with the isotropy point at T_{IP}; however, contrary to the report in [21], we observed no anomaly in χ''.

Figures 3 and 4 show the details of the low temperature anomalies for stoichiometric single crystal; the χ' and χ'' dependence upon frequency is presented in Figure 3, while Figure 4 shows how the dynamic susceptibility depends on the amplitude of the driving magnetic field H_{AC}. Clearly, the sudden drop of χ' at 28 K is reflected in the peak in χ'', and their temperature dependence does not change with frequency. By contrast, the neighboring, higher T, anomaly, manifested as a peak in χ'', does depend on the frequency. The driving field H_{AC} dependence of χ' signal is presented in Figure 5; here the real part of the susceptibility does not depend on H_{AC} above the Verwey transition, in contrast to its variation at lower temperatures. To further study the processes responsible for the χ_{AC} behavior we have cooled the stoichiometric magnetite through the transition in an external magnetic field $H = 2$ kOe parallel to [001], measuring it while applying the field, or while heating in zero field, after FC. The results are shown in Figure 6. The field cooling and subsequent heating with zero external magnetic field shifts the low temperature signal close to that at $T > T_V$, with an almost identical anomaly in the 20–60 K region. On the other hand, the signal recorded upon field cooling is diminished by a factor of almost 20. Also, the break in T_V is very small, and the low temperature signal ($T < 25$ K) is much lower than that in the T range from 50 to 120 K, with the simultaneous disappearance of the 50 K anomaly. The temperature dependence of the low T anomaly for $x = 0.0072$ is shown at several frequencies (Fig. 7), and excitation fields (Fig. 8). The anomaly is moved to lower T and its shape is definitely changed as compared to stoichiometric magnetite: the most prominent feature is the absence of the frequency-independent portion visible in Figure 3. The high temperature part ($T > 20$ K) of the $\chi'(T)$ relation is qualitatively similar to that of stoichiometric magnetite: the rise at 65 K in χ' observed in Fe_3O_4 is now moved to lower T, ca. 30 K, exhibiting a typical sigmoidal shape and

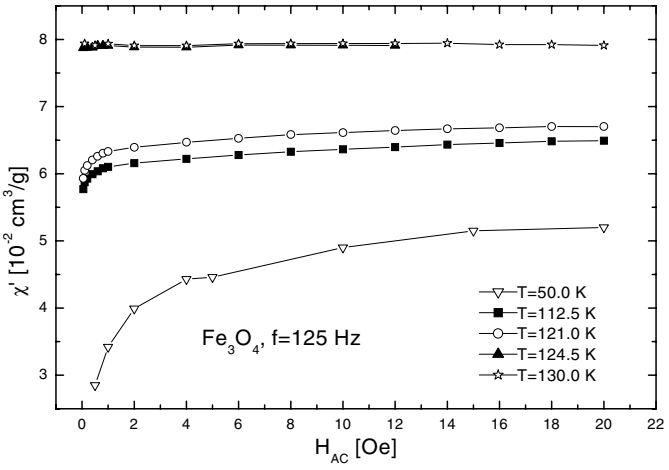

Fig. 5. χ' dependence on the amplitude of driving field H_{AC} for stoichiometric magnetite. Only the data for selected temperatures are shown.

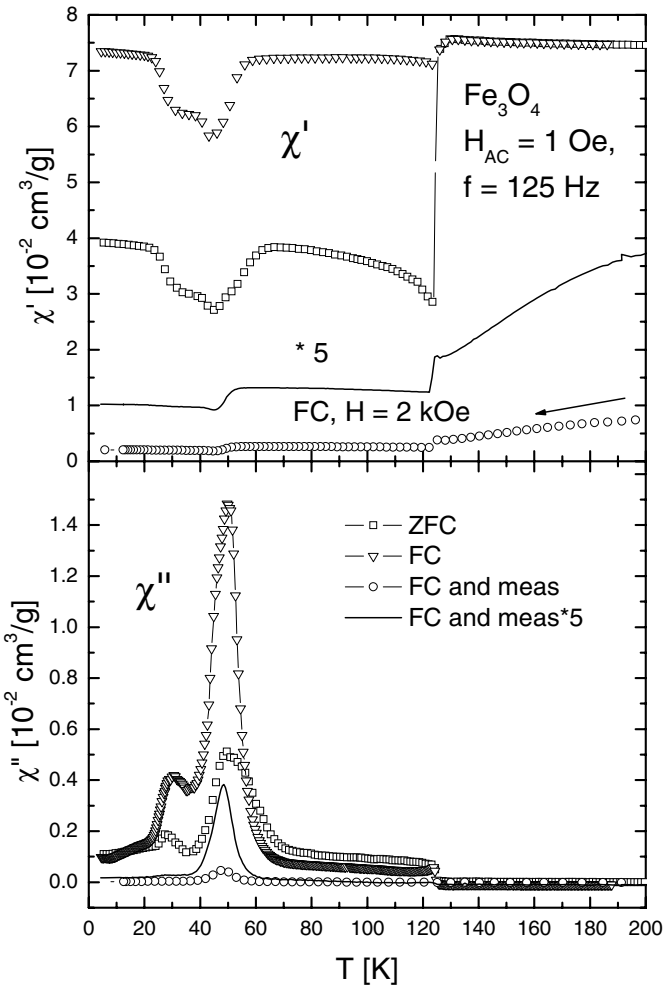

Fig. 6. χ_{AC} for stoichiometric magnetite under different cooling and measuring cycles. "ZFC" and "FC" refer to measurements performed after the samples were cooled in the relevant manner, while "FC H = 2 kOe" means that the sample was cooled down and measured simultaneously.

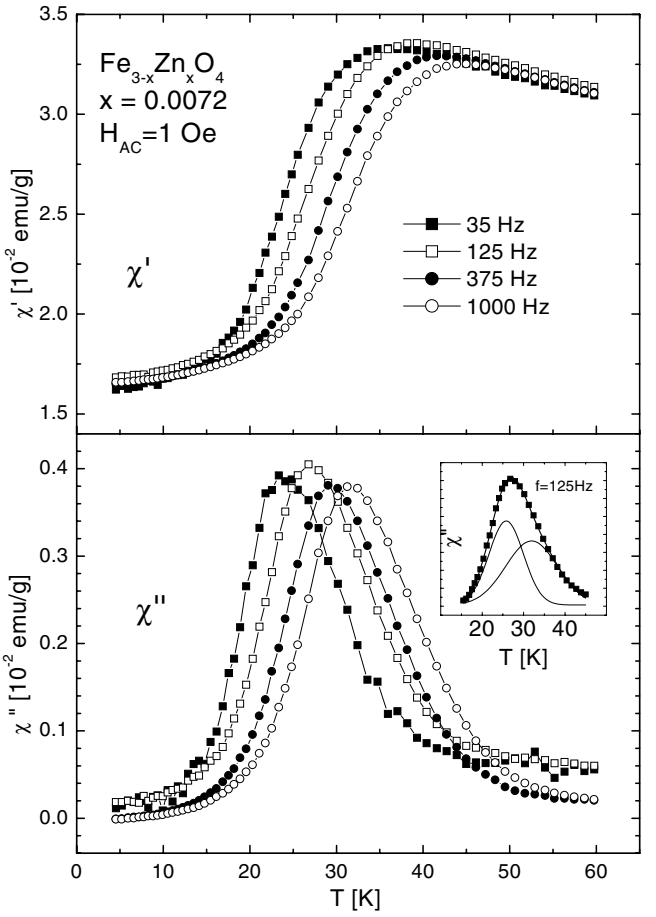

Fig. 7. Frequency dependence of χ_{AC} for $x = 0.0072$. The inset shows the example how the peak in χ'' is broken into two Gaussians.

a peak in χ''. When the H_{AC} amplitude exceeds 5 Oe, the high χ' signal is triggered, with a simultaneous build-up of χ''. For stoichiometric magnetite a similar (although gradual) increase of χ' with H_{AC} was detected in Figure 4, but the out-of-phase susceptibility was suppressed. The low temperature anomaly for $x = 0.0174$ is presented in Figures 9 and 10; again, as in stoichiometric magnetite (and also, although to less extent, in the sample $x = 0.0072$) the anomaly is split into two peaks that both move to higher T with increasing frequency f. Experimental data for $x = 0.049$ sample are shown in Figure 11; the measurement conditions are given in the figure. The low temperature anomaly is now present only in χ''. Field cooling greatly accentuates the transition, contrary to the case of stoichiometric magnetite; also, the in-field measurement does not appreciably change the character of the transition, again in contrast to Fe_3O_4.

4 Discussion

4.1 The mechanism

The basic mechanism responsible for the many effects encountered in our results appears to be the magnetic

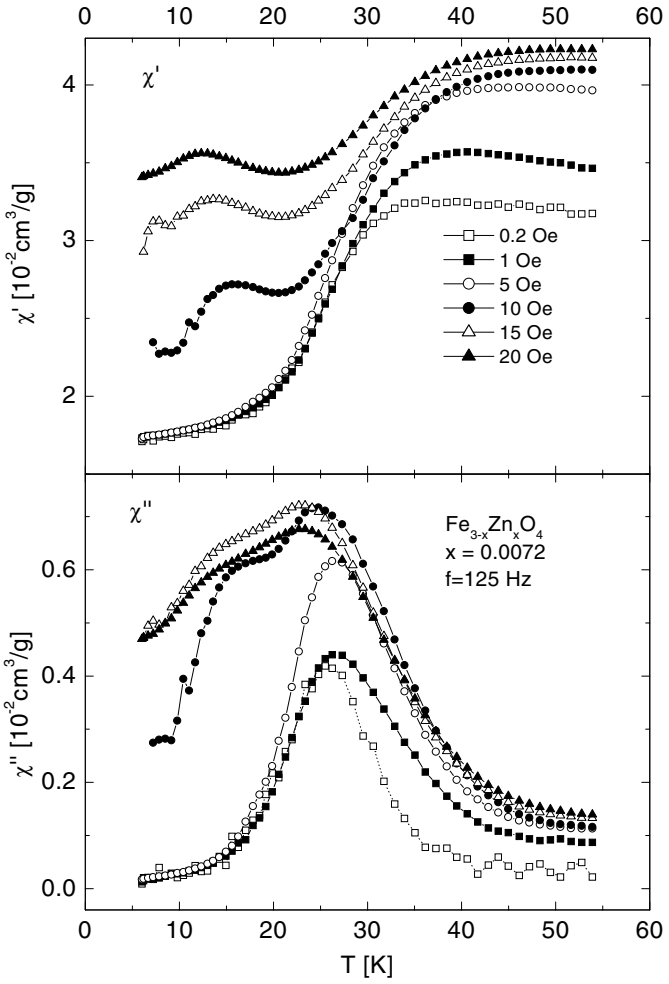

Fig. 8. H_{AC} dependence of χ_{AC} for $x = 0.0072$.

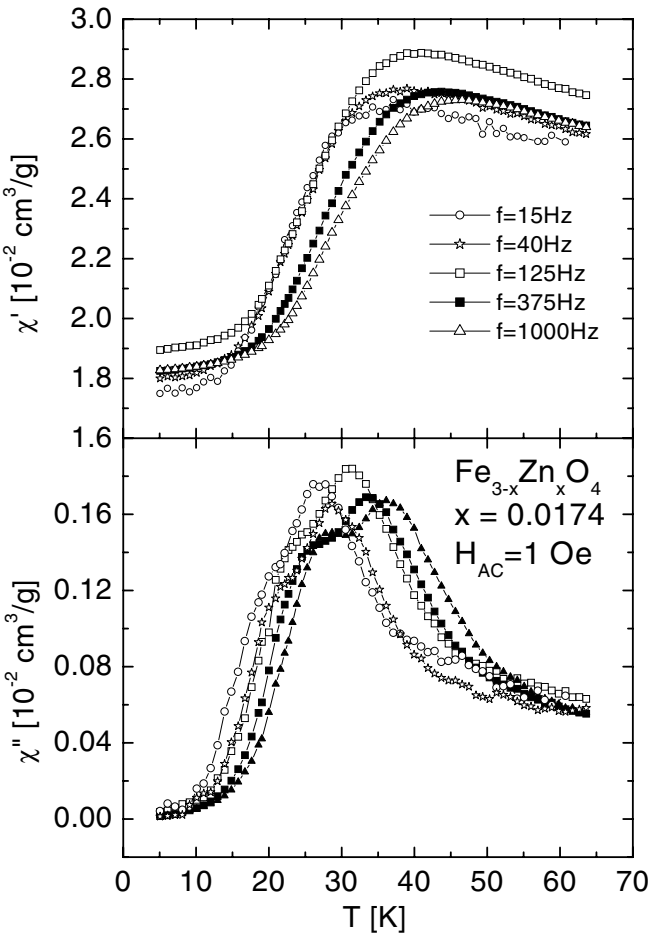

Fig. 9. Frequency dependence of χ_{AC} for $x = 0.0174$.

domain wall displacement (DWD), together with the associated relaxation processes, and the interaction of magnetic with structural domains. This conjecture, elaborated in the next section, is primarily based on the estimation of the χ' signal derived from the DWD, as specified by the relation [26]:

$$\chi_{DWD} = \frac{2M_s^2}{K_u}\frac{d}{D} \tag{1}$$

where:
M_s is the saturation magnetization (97.8 emu/g, i.e. 512 emu/cm^3 [14]);
K_u is the uniaxial anisotropy constant (20×10^5 erg/cm^3 below T_V [14]);
d is the magnetic domain wall thickness (ca. 300 nm [27]); and D is the domain size (2–3 μm [28]).

Insertion of these values leads to a χ' of the order of 10^{-3} – 10^{-2}, close to our results. The experimental results for $T > T_V$ shown in Figure 1 at least are not in conflict with this mechanism. The compressed pellet of stoichiometric magnetite exhibits a much higher χ' signal, presumably because of its highly distorted structure. This distortion produces smaller magnetic domains, thus giving rise to higher χ_{DWD}, in agreement with the above expression.

In addition, the temperature locations and character of anomalies, for the case of stoichiometric magnetite, resemble those reported in the MAE measurements [2,29]. Since the MAE was linked primarily to relaxation processes connected with the DWD we have additional confirmation that this is the dominant mechanism for the temperature and frequency/excitation magnetic field dependence of the susceptibility.

Finally, the subtleties in the T, f, and H_{AC} dependence of χ' change somewhat from one experimental run to another, similar to the characteristics of magnetic domains in all magnetic materials and structural domains, in magnetite in particular [30]. This point needs additional comment. One usually attempts to find a universal mechanism of the physical processes under consideration, here, the anomalies in susceptibility and its dependence on H_{AC}, frequency, composition, cooling, and measurements procedure. However, since many effects below the Verwey transition affect the magnetic, structural and ferroelectric domains, giving rise to interaction between all of them, and acting on those domains individually, a unique mechanism for all these effects might not emerge in this case. Hence, we concentrate below mainly on the major

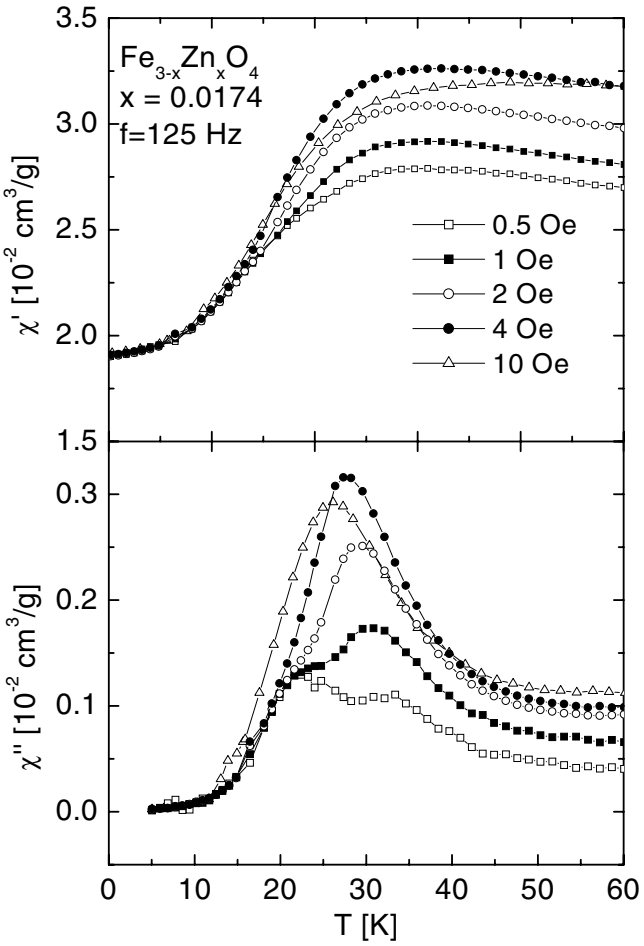

Fig. 10. H_{AC} dependence of χ_{AC} for $x = 0.0174$.

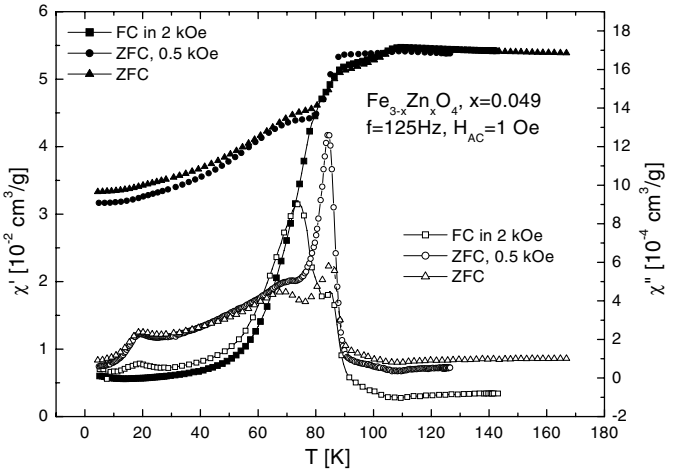

Fig. 11. Temperature dependence of χ_{AC} for $x = 0.049$ for different heat treatment and measuring conditions (solid symbols – χ', open symbols – χ''): FC sample was measured when heating in zero external field, while ZFC sample was measured either without field or in $H_{DC} = 0.5$ kOe.

effects with a common origin. The other effects are linked to diverse interactions that cannot be experimentally controlled or that result in domain structure which change slightly every time the experiment is repeated.

4.2 The Verwey transition

In the magnetization process the magnetic moments within a domain rearrange in such a way as to minimize their energy. Macroscopically this gives rise to the magnetic domain wall movement, if such a movement is possible, or else, to a magnetic moment rotation into the field direction. High temperature cubic magnetite has its easy, intermediate and hard axes along cubic $\langle 111 \rangle$, $\langle 110 \rangle$ and $\langle 001 \rangle$ directions, respectively; hence, if H_{AC} is small and directed along [100], magnetic domain wall movement can occur. Since the relaxation time for wall movement at those temperatures is relatively short, the wall can readily adjust to small applied H_{AC} values that increase the net magnetization, thereby producing large values of χ' and a vanishing value of χ''. Below the Verwey transition the easy axis coincides with the [001] direction, while [110] and $[\bar{1}10]$ are intermediate and hard axes. Since at T_V magnetite undergoes the structural phase transformation from the high temperature cubic to the monoclinic phase, each cubic $\langle 100 \rangle$ may become an easy axis, so that the material breaks into several kinds of twins. These twins, ferroelastic domains, are often smaller than 5 μm [30] in extent, so that their dimensions are comparable to those of magnetic domains [27]. In other words, the ferroelastic domain consists of basically one magnetic domain that cannot readily move in a small H_{AC} field because this requires the simultaneous transfer of a larger elastic energy. Thus, the resulting χ' below T_V should be considerably lower, with the loss signal χ'' considerably higher, as was observed (see Fig. 1).

Some of the twins mentioned above (the *c*-*c* twins) may be eliminated: the simplest way to force a particular [001] direction to become the unique easy axis is to apply a parallel external magnetic field $H > 2$ kOe while cooling; this procedure was applied here. Now the c axis in almost all the crystal points close to the H_{AC} field direction; the size of the structural domains is now in the range 2−100 μm [30], i.e. larger than magnetic domains. The magnetic domain walls can then move under the applied field without having to simultaneously move the twin boundaries. The susceptibility χ' should then resemble that for higher T, see Figure 6. There are, however, some twins that are not removed by the field cooling procedure. Those twins that still remain are related to possible interchange of a and b directions (a-b twins) as well as to the different way the c axis is inclined (either towards cubic [110], or towards $[\bar{1}10]$: a-a twins). There may also be additional, possibly small, ferroelastic domains arising from the reduction to the triclinic, low T symmetry [30]. The existence of all those twins cause that not the entire material responds to the H_{AC} field, i.e. χ' is slightly lower at $T < T_V$ than at $T > T_V$, as in Figure 6.

If the dynamic susceptibility is measured in an external magnetic field capable of curtailing the magnetic domain

structure (ca. 2.5 kOe when cooling through the transition with the magnetic field aligned along the easy axis) the signal should also be considerably diminished; this is observed in Figure 6 for stoichiometric magnetite. This effect not only reinforces our claim that what we observe is mainly due to magnetic domain wall movement, but also suggests that magnetic effects in the transition region are only side-effects that are not directly linked to the mechanism of the Verwey transition. In other words, even if the magnetic manifestations could be switched off, the transition would still proceeds in the same manner. This problem will be further discussed in a separate paper.

The above mechanism of the magnetic susceptibility should also be operational in doped and nonstoichiometric magnetite samples. Indeed, in all these materials the high temperature cubic symmetry turns to monoclinic at lower temperatures, unavoidably resulting in formation of twins. Accordingly, a characteristic step is seen in the χ' signal for each sample, as shown in Figure 1. However, the basic mechanism is the subtle interplay between magnetic and structural domains, and because both domains heavily depend on material purity, any change in purity may critically affect the susceptibility and its dependence upon the external magnetic field. We believe this mechanism to be the main reason why different field cooling procedures lead to phenomena, such as those in Figure 12, where no clear systematics is in evidence. The additional mechanism, usually adopted in discussions of AC susceptibility, see e.g. [31] and [32], that explains the characteristic step of χ' in the transition region is the magnetic moment rotation effect. Indeed, when the sample is cooled below T_V in the absence of an external magnetic field, several structural twins turn up that have their easy magnetization axis perpendicular to the AC field direction. In those twins, i.e. in roughly 2/3 of the material volume, the DWD process cannot be realized and the observed χ' value should be 1/3 of the value when a unique easy axis is established (i.e., for FC case). Since the actual signal is larger, see Figure 6, this may be due to the domain magnetization rotation (DMR) being as large as 1×10^{-2} cm^3/g. On the other hand, the $\langle 100 \rangle$ orientation we have adopted here is unique in that any deviation from this direction should result in more suitable conditions for magnetic domain wall displacement, so that the step in χ for any other orientation should be smaller. In particular, this should be true for the pellet; however, inspection of Figure 1 shows that in this case the step size is comparable. Also, the results of our numerous measurements of AC susceptibility for single crystalline and polycrystalline magnetite samples, aimed mainly to find samples with the desired T_V, show that the step at T_V is always as large as that for ZFC samples, displayed in Figure 6. These facts suggest that the DWD and DMR effects cannot fully explain the situation and that another mechanism, such as the interplay between DWD and the structural twins, as explained above, must also be considered.

Apart from the step in χ' at T_V, the driving field H_{AC} dependence of the susceptibility further differentiates the temperature region below and above the transition. For

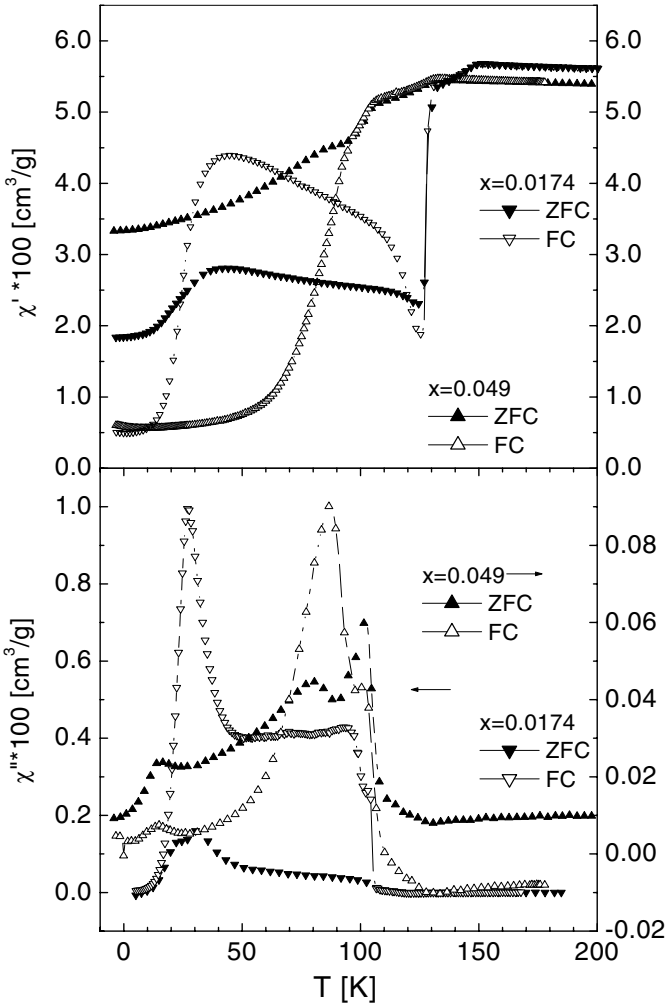

Fig. 12. Results of zero field cooling and field cooling (in $H = 2$ kOe) for $x = 0.0174$ and $x = 0.049$.

$T > T_V$ the driving field does not affect χ', while below T_V the susceptibility increases considerably with H_{AC} for low driving field amplitudes and rises linearly for $H_{AC} > 2$ Oe, as shown in Figure 5. Similar results have been obtained for field cooled sample (not shown), but the increased number of movable magnetic domain walls caused by FC produced a smaller dependence of χ' with H_{AC} at $T < T_V$, as compared to the ZFC experiment. Thus both effects: the step in χ' at T_V and the different χ' vs. H_{AC} relations below and above T_V, are correlated and related to magnetic domain wall dynamics interacting with structural domains. Additionally, the dependence of χ' on H_{AC} below T_V, indicating that the M vs. H_{AC} relation is stronger than linear, suggests that the low temperature susceptibility depends not only on changes in magnetization derived from domain walls movement, but also results from an increasing number of depinned walls. Also, the H_{AC} dependence of χ'' is consistent with this description: with growing H_{AC} more walls can be depinned and move without friction.

4.3 Anomaly at 28 K

We next discuss the fine structure in temperature dependence of susceptibility.

For stoichiometric magnetite, from the lowest possible temperatures to 25 K, χ' is rather large (Fig. 1), indicating easy and frictionless (small χ'') magnetic domain wall movements. Only a weak frequency dependence of χ' and χ'' is seen (Fig. 3), but χ' rises with increasing H_{AC} (Figs. 4 and 5), with a simultaneous decrease of χ'', as discussed above. Both the magnitude of χ' and its dependence upon H_{AC} are similar to those for 50 K $< T < T_V$, suggesting the same principal mechanism of spin motion.

The major change in $\chi(T)$ occurs at 28 K, where χ' rapidly decreases with a coincident development of the peak in χ''. A conspicuous feature of this effect is that it does not depend on frequency in the range of our experiment. Also, the anomaly can easily be removed by increasing H_{AC}: χ' levels off reaching its low T value for $H_{AC} = 10$ Oe, with a simultaneous lowering of χ'' (Fig. 4). Finally, the departure from stoichiometry, as well as even very small degrees of doping, causes χ' to become small so that the discussed anomaly (frequency independent) disappears.

The effect and the subsequent rise of χ' for $T >$ 50 K (see the next section) correspond to the relaxation anomalies observed in magnetic after effect (MAE) studies [29,33], where a time dependent (from 1 to 180 s) decrease of the initial susceptibility (i.e., the susceptibility disaccommodation) at low temperatures was reported. The MAE was explained as resulting from the relaxation of electronic states in the magnetic domain wall, so as to minimize the wall energy, i.e. to increase pinning. Two relaxation channels were proposed: incoherent tunneling of electrons from Fe^{+2} to Fe^{+3}, and intraatomic Fe^{+2} electronic excitation. The latter gives rise to a strong relaxation peak in the MAE at the same temperature where we observe the frequency-independent anomaly. The fact that the temperature of the effects, observed by MAE and AC susceptibility, match so well is suggestive.

We suggest that in the T range close to 30 K the MAE technique and the AC susceptibility probe the same electronic processes, but the manner in which these processes are triggered is different. After demagnetization (the starting point for MAE spectroscopy) the electronic processes (either incoherent tunneling or Fe^{+2} excitation) occur to minimize the magnetic, electrostatic, and elastic energy of magnetic domain wall patterns; these processes are monitored using low amplitude (few mOe) AC magnetic fields. In our measurements, with an H_{AC} field which is three orders of magnitude greater, we not only probe the ongoing processes, but can also trigger some of them (as exemplified in Figure 8, where a new phenomenon is triggered by a field of 10 Oe), i.e., intraatomic Fe^{+2} excitation. Additionally, for incoherent tunneling between Fe^{+2} and Fe^{+3} to occur, coherent tunneling, a process of much lower characteristic time is needed; this process can be investigated by our technique.

Thus, if both the relaxation peak in MAE at 30 K and our anomaly at 28 K are caused by the excitation of electronic Fe^{+2} states due to spin orbit and exchange fields [29], we would have a natural explanation why the observed process is not frequency dependent. Indeed, intraatomic electron transfers at these temperatures, if triggered by the AC field, are fast enough to follow the magnetic domain wall movement occurring ca. 15 to 1000 times per second.

For nonstoichiometric magnetite and in zinc-ferrite with $x < 0.02$, the low temperature ($T < 20$ K) frictionless wall movement (high χ'), as well as the fine structure of the anomaly at 28 K, are lost. Apparently, in accord with the above description, in samples with defects, the Fe^{+2} states are greatly disturbed and a gradual population of higher levels starts already at much lower temperatures, inaccessible in our experiment. The other possible explanation of a diminished χ', i.e. lower wall movement, is that the introduction of defects (dopant atom, vacancy) causes stronger pinning, resulting in χ' values close to zero at lowest temperatures. This suggests the existence of some ionic order in stoichiometric magnetite that is broken up by the introduction of defects.

Although the reorganization of Fe^{+2} energy levels to qualitatively explain the anomaly at 28 K may be a viable explanation some facts call this phenomenon into question. First, this process should result in an energy transfer comparable to that for thermal excitation in a two-level system; however, the shape of our χ'' peaks does not resemble the typical two-level Schottky specific heat anomaly. Also, cooling the sample in an external magnetic field of 2 kOe does not greatly affect the shape of the χ' anomaly, but accentuates the loss signal (Fig. 6). Since field cooling prevents *c*-*c* ferroelastic domain formation, as explained above, the basic explanation of the almost doubled χ' is that the number of movable magnetic domain walls has increased by a factor of two. However, the size of the anomaly at 28 K does not scale with the factor 2, as one would expect if Fe^{+2} cations within the walls were involved.

Thus, both the odd shape of χ'' peak and the behavior after FC suggest that relaxation processes at this temperatures are more subtle. On the other hand, field cooling, with the simultaneous "in field" measurement greatly broadens the effect, which indicates that the reason for this anomaly should be sought in magnetic domain formation and movement.

4.4 Anomaly at ca. 50 K

From the lowest temperatures up to 60 K stoichiometric magnetite exhibits rather strong magnetoelectric effects: the rotation of magnetization induces an electric field and vice versa [34]. Above the anomaly at 28 K, these magnetoelectric effects become more prominent. Thus, ionic order within walls starts to conform to the wall movement, initially with a time lag and later, at higher temperatures, almost instantaneously. This process may show up initially as friction in magnetic domain wall movement, resulting in a lowering of χ', with a simultaneous increase

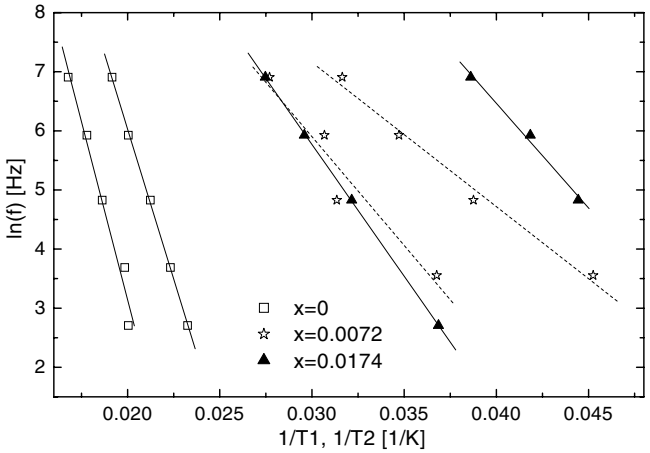

Fig. 13. Results of fitting of frequency versus the positions of two peaks, T_1 and T_2, (in which the anomaly in χ'' can be separated; see Figs. 3 and 7) according to the relation $\log(f)$ vs. $1/T$.

in χ'' and, at higher T, in an increase of χ' (the characteristic "knee" at 55 K) and a diminution of χ'', as observed around 55 K, see Figure 1. Both processes: the initial slowing down and subsequent increase of the wall movement are frequency dependent (see Fig. 3), and a linear relation $\log(f)$ vs. $1/T$ holds reasonably well, indicating a thermally activated relaxation process (see Fig. 13). Also, both processes (similar to the 28 K anomaly) are broadened in an H_{AC} field greater than 10 Oe (Fig. 4). Thus, either the number of depinned walls has increased, or the slowing effect of ionic rearrangement within domain walls, preceded by low levels mixing (a diminished anomaly at 28 K) has not taken place; both processes result in a decrease of pinning. Stoichiometric magnetite changes its properties at 55 K: above this temperature DC conduction is no longer clearly anisotropic [35], and the magnetoelectric properties described above are lost [34]. Also, for $T > 60$ K, our measurements reveal a basically featureless behavior of χ, with a value comparable to that at very low T; see Figure 1. Cooling the sample in an external DC magnetic field of 2 kOe greatly diminishes the χ' signal and changes its shape. As already mentioned, the field saturates the sample, leaving it essentially free of major magnetic domains. The small signal, see Figure 6, originates from domains that are still left. At 60 K, while lowering temperature, magnetoelectric effects set in, that result in the external magnetic field stabilizing ionic order thereby inhibiting the magnetic domain wall movement.

In doped and nonstoichiometric magnetite, apart from the changed low temperature χ' value, one still observes an increase of the wall movement resulting from the faster relaxation within domain walls, and the effect is still frequency dependent. As in stoichiometric magnetite, χ' rises with the H_{AC} amplitude at temperatures above the low T knee (i.e. when $T > 30$ K) for $0 < x < 0.02$, see Figures 8 and 10 (we did not measure the H_{AC} dependence for $x = 0.049$). On the other hand, the behavior for temperatures just below the knee is different. Here a rise in H_{AC} brings about an increase of χ', with a coincident decrease in losses for $x = 0$, while χ' stays constant for $x = 0.0072$ and 0.0174 (at $H_{AC} < 5$ Oe). With a further increase of H_{AC} yet another anomaly is triggered for $x = 0.0072$. Our attempts to separate at least two anomalies close to the knee by means of the χ'' observations are shown in Figures 3 and 7 for $x = 0$ and $x = 0.0072$, as typical examples. Plots of $1/f$ vs. $\ln(Ti)$ (T_1 refers to the lower temperature peak position, while T_2 to the higher) are presented in Figure 13. Here, an activation process $\tau = \tau_0 \exp(Q/kT)$ holds approximately, where τ $(=1/f)$ is the time after which an atomistic (i.e. small polaron [2]) jump is completed, which is attempted every τ_0 $(= 1/f_0)$ seconds. The fitted parameters for three samples are collected in Table 1, and are compared to relevant data from literature, where a similar frequency dependence of anomalies at comparable temperatures have been found.

Table 1. Fitted values of τ_0 and Q.

x: Zn content	Peak at T_1	Peak at T_2	Literature data
0	$\tau_0 = 3.8 \times 10^{-12}$ s	1.5×10^{-12} s	1×10^{-14} s
	$Q = 87$ meV	104 meV	86 meV[a]
0.0072	$\tau_0 = 5 \times 10^{-7}$ s	4.6×10^{-8} s	1.4×10^{-11} s
	$Q = 21$ meV	32 meV	70 meV[b]
0.0174	$\tau_0 = 1.1 \times 10^{-9}$ s	4.9×10^{-9} s	6.05×10^{-12} s
	$Q = 30$ meV	38 meV	65 meV[c]

[a] after [36]
[b] after [37] data for $3\delta = 0.0013$
[c] same as above, but data for $3\delta = 0.0055$

Similar relaxation effects appearing in the temperature interval 20–40 K were observed in manganese doped magnetites [38]. The peak of magnetic losses, composed of two parts, was generally interpreted as arising from fast effects occurring inside the magnetic domains, followed then by slower domain wall response, which takes place at higher T. On the other hand, in manganites, the H_{AC} field dependent χ_{AC} anomalies were explained [39] by means of the existence of magnetic clusters, i.e. the phase separation. Since in both classes of materials valence instabilities exist, this is not unreasonable that similar phase separation mechanism is operational here.

Almost no anomaly at ca. 55 K can be seen for $x = 0.049$ in χ' and only a small peak shows up in χ'', as shown in Figure 11. The results for the sample cooled in a field of 2 kOe suggest that the magnetic domain wall movement is almost completely blocked, in contrast to the behavior for stoichiometric magnetite (Fig. 6).

4.5 Other effects at higher temperatures

The comparison of ZFC and FC effects on samples with $x = 0.0174$ and $x = 0.049$ is shown in Figure 12. For $x = 0.0174$, after FC, the signal at lowest T is very small, rising dramatically at ca. 30 K. This temperature roughly

coincides with that where the real part of complex dielectric constant diverges [37], and may indicate the onset of magnetoelectric effects. The χ' signal is now greater than that for ZFC, because of the enlarged structural domains that cause free magnetic domain wall movement. The susceptibility then remains featureless up to 95 K, where it drops below that for ZFC, in contrast to the $x = 0$ behavior. This process may be linked to c axis switching, mentioned in the introduction, which may be increased by FC.

Increasing T above T_V results in χ' being almost identical for all samples (with very small χ'') over the whole measured temperature range. This signal is temperature independent at temperatures exceeding T_{IP}, the isotropy point temperature, where the anisotropy K_1 passes through zero [10] and where the magnetic easy axis changes direction from low temperature $\langle 001 \rangle$ to $\langle 111 \rangle$. This temperature is manifested by a kink in the $\chi'(T)$ relation; T_{IP} roughly scales with the Verwey temperature (see the inset in Fig. 2). The same correlation T_{IP} vs. T_V had already been inferred from the temperature dependence of the elastic constant c_{11} [40]. In both cases the rough proportionality between both pairs of anomalies suggests that the Verwey transition and the isotropy point are correlated.

4.6 Similarities to MAE measurements

As already mentioned, results qualitatively similar to ours have been observed in the Magnetic After Effect technique, even though those effects have relaxation times 10^4 higher than those observed here. The relaxation gap observed there between 30 and 50 K, i.e. at the T range where χ' drops in stoichiometric magnetite and where several anomalies are found, has been explained as a combined effect, namely the termination of octahedral Fe^{+2}-Fe^{+3} incoherent electron tunneling at $T = 30$ K, and the onset of small polaron electron hopping within octahedral Fe^{+2}-Fe^{+3} pairs. Thus, both our results and the MAE data prove the existence of relaxation effects at ca. 50 K for stoichiometric magnetite and, at lower T, for doped and nonstoichiometric samples, with a very wide relaxation time spectrum. On the other hand, the anomaly at $T = 28$ K is different since no frequency dependence was encountered, in contrast to the MAE results, where the peak depends on the observation time and shows typical relaxation behavior.

5 Conclusions

In conclusion, we have measured the temperature, frequency, and H_{AC} dependence of the AC susceptibility of zinc-doped magnetite single crystals. We have argued that magnetic domain wall displacement is mainly responsible for the majority of effects and that the usual drop in χ' at T_V results from the interplay between magnetic and structural domains formed below T_V. We have found several anomalies, manifested as drops in χ' and in the relevant peaks in absorption part χ'' in the T region from 25 to 60 K for $x = 0$ and, at lower T, for doped or nonstoichiometric magnetite. In particular, the anomaly at $T = 28$ K, observed only in stoichiometric magnetite, does not show the normal frequency dependence, contrary to the effect at 50 K. This temperature region, 25–60 K, roughly corresponds to the temperature where magnetoelectric effects are reported to disappear.

With a further increase of temperature, almost up to T_V, a gradual decrease of χ' was observed, which is probably linked to electron transfer, revealed by axis switching.

Finally, the isotropy point, seen as a kink in χ', roughly scales with the Verwey transition temperature.

This work is financially supported by the KBN State Committee for Scientific Research and was supported in part by Grant DMR 96 12130 of the National Science Foundation, USA.

References

1. A. Gupta, J.Z. Sun, J. Magn. Magn. Mat. **200**, 24 (1999)
2. F. Walz, J. Phys.: Condens. Matter **14**, R285-R340 (2002)
3. J. Garcia, G. Subias, J. Phys.: Condens. Matter **16**, R145 (2004)
4. P.W. Anderson, Phys. Rev. **102**, 1008 (1956)
5. P. Novak, H. Stepankova, J. Englich, J. Kohout, V.A.M. Brabers, Phys. Rev. B **61**, 1256 (2000)
6. J. Garcia, G. Subias, M.G. Pgoietti, J. Blasco, H. Renevier, J.L. Hodeau, Y. Joly, Phys. Rev. B **63**, 54110 (2001)
7. J.P. Wright, J.P. Attfield, P.G. Radealli, Phys. Rev. B **66**, 214422 (2002)
8. M.P. Pasternak, W.M. Xu, G.Kh. Rozenberg, R.D. Taylor, R. Jeanloz, J. Magn. Magn. Mat. **265**, L107 (2003)
9. Z. Szotek, W.M. Temmerman, A. Svane, L. Petit, G.M. Stocks, H. Winter, Phys. Rev. B **68**, 054415 (2003)
10. R. Aragón, Phys. Rev. B **46**, 5334 (1992)
11. R. Aragón, Phys. Rev. B **46**, 5328 (1992)
12. S. Chikazumi, AIP Conf. Proc. **29**, 382 (1975)
13. Z. Kąkol, J. Sabol, J.M. Honig, Phys. Rev. B **43**, 649 (1991)
14. Z. Kąkol, J.M. Honig, Phys. Rev. B **40**, 9090 (1989)
15. B.A. Calhoun, Phys. Rev. **94**, 1577 (1954)
16. J.P. Shepherd, J.W. Koenitzer, R. Aragón, J. Spałek, J.M. Honig, Phys. Rev. B **43**, 8461 (1991)
17. P. Wang, Z. Kąkol, M. Wittenauer, J.M. Honig, Phys. Rev. B **42**, 4553 (1990)
18. H.P.J. Wijn, H. van der Heide, Rev. Mod. Phys. **25**, 98 (1953)
19. V. Skumryev, J. Nogues, J.S. Munoz, B. Martinez, R. Senis, J. Fontcuberta, L. Pinsard, A. Revcolevsci, Y.M. Mukovskii, Phys. Rev. B **62**, 3879 (2000)
20. J. Garcia, J. Blasco, M.C. Sanchez, M.G. Proietti, G. Subias, Surf. Rev. Lett. **9**, 821 (2002)
21. V. Skumryev, H.J. Blythe, J. Cullen, J.M.D. Coey, J. Magn. Magn. Mat. **196-197**, 515 (1999)
22. M. Bałanda, A. Wiecheć, Z. Kąkol, A. Kozłowski, D. Kim, J.M. Honig, Acta Phys. Pol. B **34**, 1513 (2003)

23. H.R. Harrison, R. Aragón, Mater. Res. Bull. **13**, 1097 (1978)
24. R. Aragón, H.R. Harrison, R.H. McCallister, C.J. Sandberg, Cryst. Growth. **61**, 221 (1983)
25. Z. Kąkol, A. Kozłowski, Sol. St. Sciences **2**, 737 (2000)
26. A.H. Groenendijk, A.J. Van Duyneveldt, R.D. Willet, Physica B **101**, 320 (1980)
27. K. Moloni, B.M. Moskowitz, E.D. Dahlberg, Geophysical Res. Lett. **23**, 2851 (1996)
28. T.G. Pokhil, B.M. Moskowitz, J. Appl. Phys. **79**, 6064 (1996)
29. F. Walz, M. Weidner, H. Kronmüller, Phys. St. Sol. (a) **59**, 171 (1980)
30. C. Medrano, M. Schlenker, J. Baruchel, J. Espeso, Y. Miyamoto, Phys. Rev. B **59**, 1185 (1999)
31. X.C. Kou, R. Grössinger, G. Hilscher, H.R. Kirchmayer, Phys. Rev. B **54**, 6421 (1996)
32. D.-X. Chen, V. Skumryev, H. Kronmüller, Phys. Rev. B **46**, 3496 (1992)
33. H. Kronmüller, F. Walz, Phil. Mag. B **42**, 433 (1980)
34. T. Inase, Y. Miyamoto, J. Phys. Soc. Jpn **56**, 3683 (1987)
35. S. Chikazumi, AIP Conf. Proc **29**, 382 (1975)
36. M. Kobayashi, Y. Akishige, E. Sawaguchi, J. Phys. Soc. Jpn **55**, 4044 (1986)
37. M. Kobayashi, Y. Akishige, E. Sawaguchi, J. Phys. Soc. Jpn **57**, 3474 (1988)
38. N. Yamada, S. Iida, J. Phys. Soc. Jpn **24**, 952 (1968)
39. V. Skumryev, J. Nogues, J.S. Munoz, B. Martinez, R. Senis, J. Fontcuberta, L. Pinsard, A. Revcolevsci, Y.M. Mukovskii, Phys. Rev. B **62**, 3879 (2000)
40. Z. Kąkol, A. Kozłowski, M. Bałanda, H. Schwenk, B. Lüthi, J.M. Honig, *Proc. 8th. Int. Conf. On Ferrites, Kyoto, Jpn. Soc. Powder and Powder Metallurgy 2000*, pp. 126–130, edited by M. Abe, Y. Yamazaki (The Japan Society of Powder and Powder Metallurgy, 2000)